Materials Science Forum Vols. 727-728 (2012) pp 80-84
Online available since 2012/Aug/24 at www.scientific.net

doi:10.4028/www.scientific.net/MSF.727-728.80

Microstructure and Electrochemical Properties of a LaMgAlMnCoNi Based Alloy for Ni/MH Batteries

E. A. Ferreira[1,a], J. M. Serra [2,b], J. C. S. Casini [1,c], H. Takiishi [1,d], R. N. Faria [1,e]

[1] Energy and Nuclear Research Institute, IPEN/CNEN-SP, Av. Prof. Lineu Prestes, 2242,ZIP 05508-000, São Paulo, Brazil
[2] Instituto de Tecnología Química, Universidad Politécnica de Valencia-Consejo Superior de Investigaciones Científicas, Av.de los Naranjos s/n, 46022 Valencia, Spain
[a] eaferreira@ipen.br, [b] jmserra@itq.upv.es,[c] jcasini@ipen.br, [d] takiishi@ipen.br; [e] rfaria@ipen.br

Keywords: La-Mg-Ni, hydrogen storage alloy, structures, properties.

Abstract. The microstructure and electrochemical properties of a $La_{0.7}Mg_{0.3}Al_{0.3}Mn_{0.4}Co_{0.5}Ni_{3.8}$ hydrogen storage alloy have been studied. The anode was prepared using a mixture of the ingot alloy in the as-cast state with carbon black and polytetrafluoroethylene (PTFE) as a binder. A $Ni(OH)_2$ electrode was used as the cathode of the square-type test cell. A separator was used together with a 6M KOH electrolyte. Microstructure and phase composition of the alloy have been investigated using inductively coupled plasma – atomic emission spectrometry (ICP-AES), scanning electron microscopy (SEM), energy dispersive X-ray analysis (EDX) and X-ray diffraction analysis (XRD). A niobium-containing alloy has also been included for a comparison.

Introduction

Since the discovery of the hydride-forming metals, many applications have been considered. Until now, the most popular of these applications is still hydrogen storage in Ni/MH batteries. However, to keep Ni/MH batteries competitive to other power sources, enhanced performances need to be obtained by developing new generation of compounds [1-6]. In the last years, much attention was paid to the La–Ni system. Rare earth-based AB_5-type alloys have been exploited as negative electrode materials in commercial Ni/MH cells, where A is a rare earth and B a transition metal [7,8].Because Co is costly, AB_5 alloys of the type $La_{0.7}Mg_{0.3}Al_{0.3}Mn_{0.4}X_{0.5}Ni_{3.8}$ (X= Co,Nb) with modification in the B part were used for this study.

Experimental

Commercial alloys in the as-cast state were studied in this work. The chemical analysis by ICP-AES of the cast alloys is given in Table 1.

Table 1 - Composition by ICP-AES in the $La_{0.7}Mg_{0.3}Al_{0.3}Mn_{0.4}X_{0.5}Ni_{3.8}$ (X= Co,Nb) alloys

Nominal Composition and Substitution Composition [at.%]	Specified and Analyzed Composition [wt.%]						
	La	Mg	Al	Mn	Co	Nb	Ni
$La_{0.7}Mg_{0.3}Al_{0.3}Mn_{0.4}Co_{0.5}Ni_{3.8}$	25.12	1.88	2.09	5.68	7.61	--	57.62
$La_{0.7}Mg_{0.3}Al_{0.3}Mn_{0.4}Nb_{0.5}Ni_{3.8}$	24.06	1.80	2.00	5.54	--	11.50	55.20

In order to prepare the battery the following procedure was adopted. Five grams of the cast $La_{0.7}Mg_{0.3}Al_{0.3}Mn_{0.4}X_{0.5}Ni_{3.8}$ (X= Co,Nb) alloy was crushed with a mortar and pestle in air, such that all the material passed through a < 44 μm sieve. The powder (140 mg) was mixed with graphite and PTFE (140 mg) and pressed into a small electrode (approximately 2x2 cm^2; 1 mm thick).Separator and positive electrode ($Ni(OH)_2$) were taken from a commercial battery. At the charge/discharge cycle tests, the charge was conducted using the current 14 mA during 5 hours and discharge at 7mA until voltage reached -0.9 V.

Results and Discussion

The chemical compositions of the phases, analyzed using EDX on a SEM in the as-cast alloy, are presented in Table 2 and 3. The $La_{0.7}Mg_{0.3}Al_{0.3}Mn_{0.4}X_{0.5}Ni_{3.8}$ (X= Co,Nb) alloy is composed mainly of the matrix phase and other phases in the grain boundaries. Rare earth (RE) content in the matrix phase was about 18-16 at.%. Elements as Al, Mn and Co are found inside the matrix phase which showed a RE:(Al, Mn, Co, Ni) atomic ratio of approximately 5, indicating a 1:5-type phase. The as-cast microstructures by SEM of the alloys with a typical grain structure are shown in Fig.1.

Table 2 - Composition by EDX in the $La_{0.7}Mg_{0.3}Al_{0.3}Mn_{0.4}Co_{0.5}Ni_{3.8}$ alloy

Phase	Analyzed Composition [wt.%]					
	La	Mg	Al	Mn	Co	Ni
Matrix (M)	16.7 ±0.4	--	1.0 ±0.6	2.1 ±0.2	7.7 ±0.5	72.3 ±0.2
Gray (G)	9.0 ±0.3	5.1±0.2	1.3±0.3	8.9±0.3	8.5 ±0.2	66.9 ±0.3
Black (B)	<1	2.0±0.3	7.4±0.5	20.7±0.4	8.5 ±0.2	60.4±0.4
Dark Gray (DG)	< 1	< 1	3.9 ±0.3	16.3±0.1	17.4±0.3	61.5 ±0.1

Table 3 - Composition by EDX in the $La_{0.7}Mg_{0.3}Al_{0.3}Mn_{0.4}Nb_{0.5}Ni_{3.8}$ alloy

Phase	Analyzed Composition [wt.%]					
	La	Mg	Al	Mn	Nb	Ni
Matrix (M)	18.2 ±0.6	--	4.6 ±0.3	11.3 ±0.3	-	65.8 ±0.2
Dark Gray (G)	--	--	--	1.2 ±0.4	19.4 ±0.5	79.3 ±0.3
White(W)	38.1 ±0.5	8.3 ±0.2	--	2.7 ±0.2	--	50.8 ±0.2

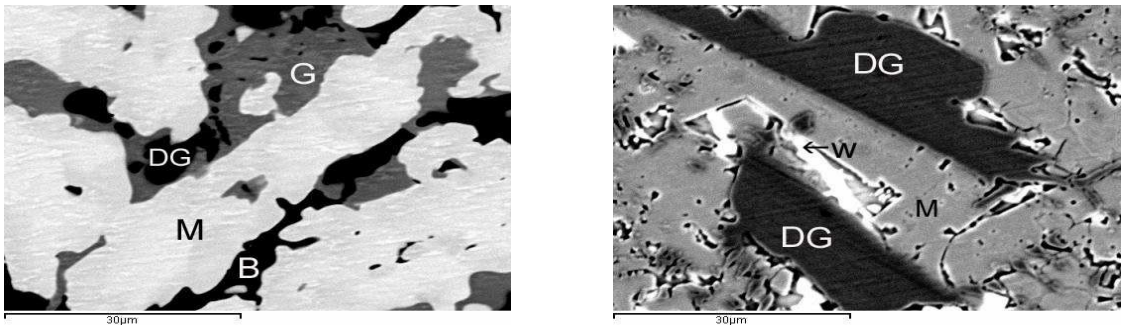

(a) (b)

Fig. 1 - Backscattered electron image of the as-cast microstructure (2000x): (a) $La_{0.7}Mg_{0.3}Al_{0.3}Mn_{0.4}Co_{0.5}Ni_{3.8}$ and (b) $La_{0.7}Mg_{0.3}Al_{0.3}Mn_{0.4}Nb_{0.5}Ni_{3.8}$

X-ray diffraction patterns of $La_{0.7}Mg_{0.3}Al_{0.3}Mn_{0.4}X_{0.5}Ni_{3.8}$ (X= Co,Nb) alloys are presented Fig.2 ($La_{0.7}Mg_{0.3}Al_{0.3}Mn_{0.4}Co_{0.5}Ni_{3.8}$) and Fig.3 ($La_{0.7}Mg_{0.3}Al_{0.3}Mn_{0.4}Nb_{0.5}Ni_{3.8}$). The Crystallographica Search-Match software (CSM) and PowderCell 2.3 software were used to determine the phase relationships. The alloys are multi-phases, mainly including $LaNi_5$, $(La,Mg)Ni_3$ and $NbNi_3$ phases. The lattice parameters and the phases abundances of the alloys are tabulated in Table 4. It shows that the main phases of the alloys are $CaCu_5$-type hexagonal $LaNi_5$ phase and $PuNi_3$-type rhombohedral $(La,Mg)Ni_3$ phase. After total substitution of Co with Nb, the intensity of the $LaNi_5$ peaks decreases and the intensity of the $(La,Mg)Ni_3$ peaks increases.

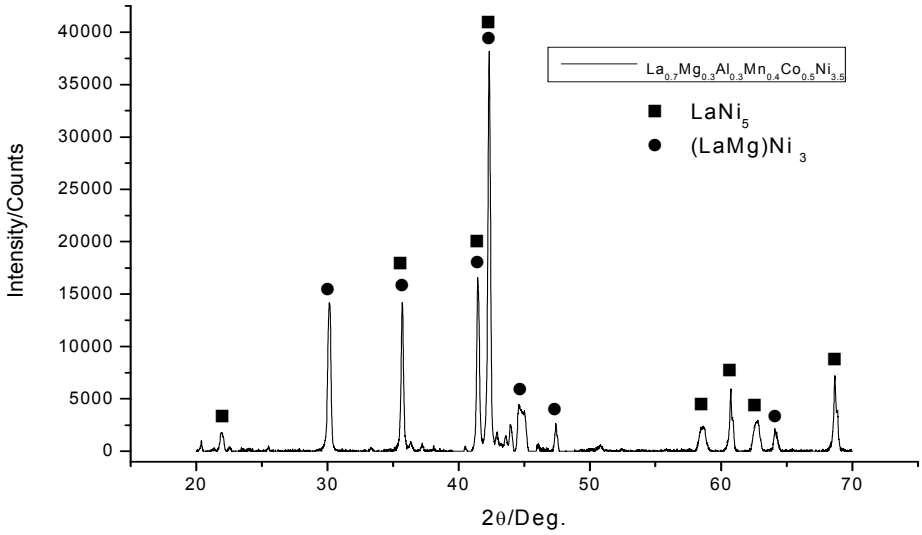

Fig. 2 - X-ray diffraction patterns of the $La_{0.7}Mg_{0.3}Al_{0.3}Mn_{0.4}Co_{0.5}Ni_{3.8}$

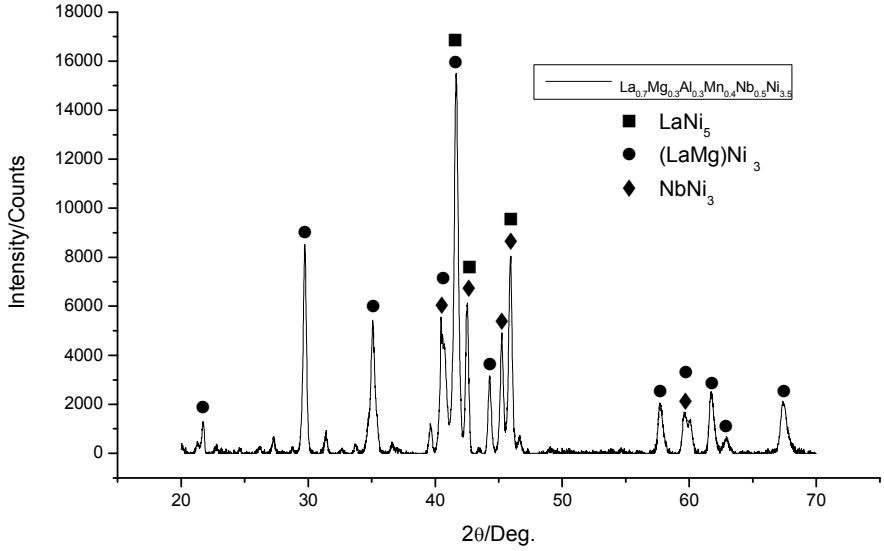

Fig. 3 - X-ray diffraction patterns of the $La_{0.7}Mg_{0.3}Al_{0.3}Mn_{0.4}Nb_{0.5}Ni_{3.8}$

Table 4 - Characteristics of structural parameters of main phases in the alloys

Alloys	**Phases**	**Lattice parameter [Å]**		**Phase Abundance**
		a	**c**	**[wt.%]**
$La_{0.7}Mg_{0.3}Al_{0.3}Mn_{0.4}Co_{0.5}Ni_{3.8}$	$LaNi_5$	5.067	4.036	62.12
	$(LaMg)Ni_3$	5.065	24.341	37.88
$La_{0.7}Mg_{0.3}Al_{0.3}Mn_{0.4}Nb_{0.5}Ni_{3.8}$	$LaNi_5$	5.076	4.047	47.90
	$(LaMg)Ni_3$	5.098	24.596	39.87
	$NbNi_3$	5.104	4.553	12.23

The discharge capacity plotted versus cycle number of the battery is shown in Fig 3. The negative electrode, produced with a $La_{0.7}Mg_{0.3}Al_{0.3}Mn_{0.4}Co_{0.5}Ni_{3.8}$ cast alloy, exhibited an excellent performance and a maximum discharge capacity of 324 $mAhg^{-1}$ (twelfth cycle). The electrode, produced with a $La_{0.7}Mg_{0.3}Al_{0.3}Mn_{0.4}Nb_{0.5}Ni_{3.8}$ cast alloy, was activated quickly (eleventh cycle) but exhibited a lower maximum discharge capacity of 221 $mAhg^{-1}$. The cycle number dependence of discharge capacity of the alloys is illustrated in Fig. 4.

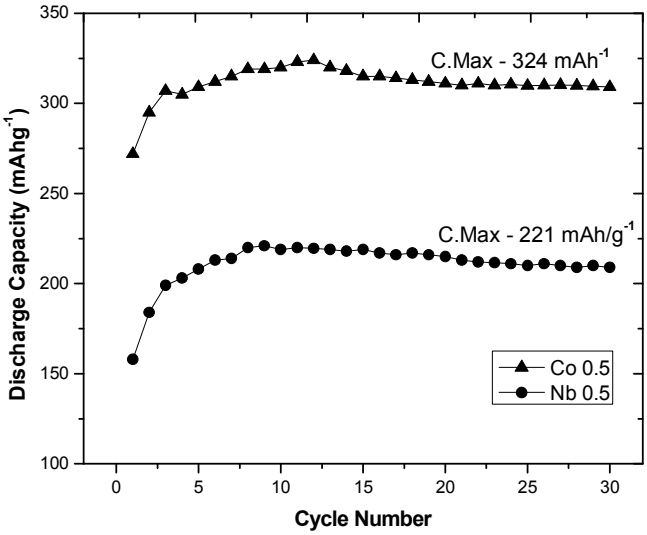

Figure 4 - Cycle number dependence of the discharge capacity of the alloys

The activation capability was characterized by initial activation number. The initial activation number was defined as the number of cycle required for attaining maximum discharge capacity through charge-discharge cycle. The maximum discharge capacity curves for the $La_{0.7}Mg_{0.3}Al_{0.3}Mn_{0.4}X_{0.5}Ni_{3.8}$ (X= Co,Nb) alloys are show in Fig. 5a ($La_{0.7}Mg_{0.3}Al_{0.3}Mn_{0.4}Co_{0.5}Ni_{3.8}$ - twelfth cycle) and Fig.5b ($La_{0.7}Mg_{0.3}Al_{0.3}Mn_{0.4}Nb_{0.5}Ni_{3.8}$ - eleventh cycle).

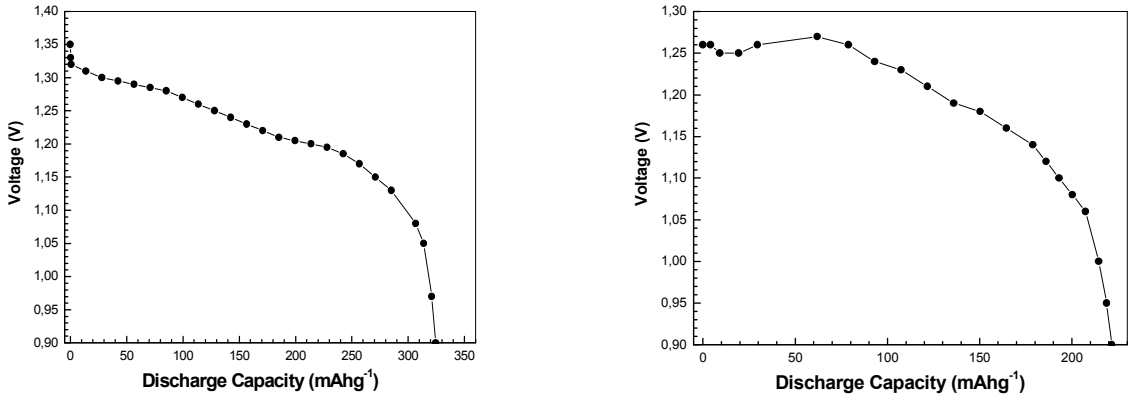

(a) (b)

Figure 5 - The maximum discharge capacity curves: (a) $La_{0.7}Mg_{0.3}Al_{0.3}Mn_{0.4}Co_{0.5}Ni_{3.8}$ - twelfth cycle and (b) $La_{0.7}Mg_{0.3}Al_{0.3}Mn_{0.4}Nb_{0.5}Ni_{3.8}$ - eleventh cycle.

The best activation capability of the alloy $La_{0.7}Mg_{0.3}Al_{0.3}Mn_{0.4}Nb_{0.5}Ni_{3.8}$ mainly ascribe to their multiphase constitution because the phase boundary among $LaNi_5$, $(La,Mg)Ni_3$ and $NbNi_3$ phases decreases lattice distortion and strain energy formed during the process of hydrogen

absorption/desorption. Moreover, phase boundary provides good tunnels for diffusion of hydrogen atoms. The results in Fig. 5a and 5b also show that with the total substitution of Co for Nb, the maximum discharge capacity of the decreases from 324 $mAhg^{-1}$ to 221 $mAhg^{-1}$. This is because that substitution of Co with Nb decreases enthalpy of hydrogenation reaction and plateau pressure of hydrogen desorption, and improves thermal stability of the hydride. The partially absorbed hydrogen atoms of the alloy electrodes cannot be effectively released [9]. Therefore, the capability of reversible hydrogen storage decreases with increasing Nb content.

Conclusions

The $La_{0.7}Mg_{0.3}Al_{0.3}Mn_{0.4}Co_{0.5}Ni_{3.8}$ cast alloy, exhibited an excellent performance and a maximum discharge capacity of 324 $mAhg^{-1}$. The electrode, produced with a $La_{0.7}Mg_{0.3}Al_{0.3}Mn_{0.4}Nb_{0.5}Ni_{3.8}$ cast alloy, was activated quickly but exhibited a lower maximum discharge capacity of 221 $mAhg^{-1}$. The substitution of Co with Nb in the LaMgAlMnCoNi-based alloys reduced electrochemical kinetics property of negative electrodes.

Acknowledgements

The authors wish to thank CAPES, CNPQ, IPEN-CNEN/Brazil, Euro Brazilian Windows II (EBW II) and the Universidad Politécnica de Valencia (UPV- CSIC- Spain) for the financial support and infrastructure made available to carry out this investigation.

References

[1] F. Feng, M. Geng and D.O. Northwood: International Journal of Hydrogen Energy Vol.26 (2001), p.725.
[2] A.K. Shukla, S. Venugopalan and B. Hariprakash: Journal of Power Sources Vol.100 (2001), p. 125.
[3] K. Hong: Journal of Alloys and Compounds Vol. 321(2001), p. 307.
[4] H. Pan, Q. Jin, M. Gao, Y. Liu, R. Li and Y. Lei: Journal of Alloys and Compounds Vol. 373 (2004), p. 237.
[5] H. Pan, X. Wu, M. Gao, N. Chen, Y. Yue and Y. Lei: International Journal of Hydrogen Energy Vol. 31 (2006), p. 517.
[6] T. Ozaki, H.B. Yang, T. Iwaki, S. Tanase, T. Sakai, H. Fukunaga, N. Matsumoto, Y. Katayama, T. Tanaka, T. Kishimoto and M. Kuzuhara: Journal of Alloys and Compounds Vols. 408-412 (2006), p. 294.
[7] H. Pan, N. Chen, M. Gao, R. Li, Y. Lei and Q. Wan: J. Alloys and Comp. Vol. 397 (1-2) (2005), p. 306.
[8] Y.F. Liu, H.G. Pan, R. Li and Y.Q. Lei: Materials Science Forum Vol. 473-470 (2005), p. 2457.
[9] R. Tang, Y.N. Liu, C.C. Zhu, J.W. Zhu and G. Yu: Intermetallic Vol. 361(4) (2006), p 14.

Advanced Powder Technology VIII
10.4028/www.scientific.net/MSF.727-728

Microstructure and Electrochemical Properties of a LaMgAlMnCoNi Based Alloy for Ni/MH Batteries
10.4028/www.scientific.net/MSF.727-728.80